Pergamon

J. Mech. Phys. Solids, Vol. 42, No. 6, pp. 897–911, 1994
Elsevier Science Ltd
Printed in Great Britain
0022–5096/94 $7.00 + 0.00

0022–5096(94)E0005–O

CAVITY AND DISLOCATION INSTABILITY DUE TO ELECTRIC CURRENT

W. YANG

Department of Engineering Mechanics, Tsinghua University, Beijing 100084, China

and

W. WANG and Z. SUO

Mechanical and Environmental Engineering Department and Materials Department, University of California, Santa Barbara, CA 93106, U.S.A.

(*Received* 28 *October* 1993; *in revised form* 16 *January* 1994)

ABSTRACT

AN ELECTRIC CURRENT drives atomic diffusion in aluminum lines. The phenomenon, known as electromigration, has been a persistent problem in integrated circuits, as the current density increases and the linewidth shrinks for every new generation of the technology. As atoms diffuse, cavities nucleate, enlarge and migrate. Evidence has accumulated that an aluminum line often fails when a rounded cavity collapses into a narrow slit across the width of the line. The fatal slits are often found to be transgranular, i.e. each slit cuts across a single grain. We investigate theoretically this instability phenomenon. Because the shape changes in a relatively short time below half the melting temperature of aluminum, atoms are assumed to diffuse only along the cavity surface, under the combined action of the electron wind and surface tension. When subjected to a small electric field, a circular cavity migrates as atoms diffuse from one portion of the cavity surface to another; the cavity remains circular, so that capillarity does not drive diffusion. However, the cavity buckles above a critical electric field, elongating either along or normal to the electric field. The surface tension now drives the atomic diffusion to restore the circular shape. The instability sets in if the electric field prevails over the surface tension. The general problem is formulated in terms of nonlinear differential equations, and the pre-bifurcation, bifurcation and post-bifurcation solutions are discussed. In addition, we analyse an analogous phenomenon: a prismatic dislocation loop climbs due to core diffusion driven simultaneously by the electron wind and line tension. The climb relocates mass at relatively low temperatures and thereby degrades the aluminum lines.

1. INTRODUCTION

WHEN CURRENT FLOWS in an aluminum line, the electron wind causes the atoms to diffuse in the direction of the electron flow. The phenomenon, known as electromigration, has been a persistent problem in integrated circuits (HO and KWOK, 1989; TOTTA, 1991; THOMPSON and LLOYD, 1993). Cavities nucleate and grow as atoms diffuse, leading to open failure. Empirically, electrical resistance is monitored with time, and the lifetime determined when the resistance becomes infinite. Electric fields and temperatures higher than service conditions accelerate the tests. The lifetime under the service conditions is extrapolated using an empirical formula.

Although valuable in circuit design, the extrapolation has revealed little of the

underlying physical processes. The lack of a basic understanding has many unfortunate consequences. First, interconnects under accelerated and service conditions may fail in different ways, in which case the extrapolation is either unsafe or overly conservative. Second, the knowledge gained for wide polycrystalline lines does not readily apply to submicron interconnects as the linewidth shrinks and the microstructure changes. Third, the empirical approach sheds no light on the search for better interconnect alloys.

Recent microscopy studies have focussed on the sequence of events leading to failure. Silicon is a good heat dissipater, so that the aluminum interconnects in service operate below, say, 400 K. At such temperatures, diffusion through the lattice is negligible compared to diffusion along grain boundaries, surfaces, interfaces and dislocation cores. The aluminum melting temperature being $T_M = 933$ K, the relevance of high temperature experiments is questionable. In this paper, we will only quote from experiments below 500 K. Attention is focussed on cavities, following their *nucleation*, *growth*, *migration* and *shape change*. GENUT *et al.* (1991) showed that a cavity can nucleate at a grain boundary triple junction. Similarly, in a bamboo-like line a cavity can nucleate at a junction of a grain boundary and an aluminum–passivation interface. Cavity growth is readily observed, or inferred, because open failure is associated with a cross-linewidth cavity. Cavities were observed to migrate in single crystal lines (SHINGUBARA and NAKASAKI, 1991), and to penetrate grain boundaries in bamboo-like lines (KRAFT *et al.*, 1993). Slit-like cavities were discovered by SANCHEZ *et al.* (1992) in unpassivated lines, by ROSE (1992) in passivated lines, and by JOO and THOMPSON (1993) in unpassivated single crystal lines. In a sequence of pictures, KRAFT *et al.* (1993) showed that a rounded cavity grows, migrates, changes its shape and finally collapses into a slit that causes open failure.

Theoretical investigations have followed the same sequence of events. Cavity nucleation and growth have been studied by many investigators (e.g. ARZT and NIX, 1991; KIRCHHEIM, 1992; KORHONEN *et al.*, 1993; LLOYD, 1991), but models studied so far are not realistic enough to predict the microscopic processes. A good theory would identify diffusion paths, driving forces and atomic sinks. Lattice diffusion being negligible, a cavity can grow only if it is connected by fast diffusion paths to atomic sinks. Furthermore, whether a cavity will grow or shrink depends on whether the electron wind or the capillary force prevails. Cavity migration is understood in terms of surface diffusion (HO, 1970; LI *et al.*, 1992). The cavity surface has high diffusivity because the interconnects are uncontaminated, being encased in passivations or native oxide scales. Atoms diffuse on the cavity surface from one portion of the cavity to another, so that the cavity migrates in a crystal lattice without changing its shape. KRAFT *et al.* (1993) recognized that a slight asymmetry in the cavity shape can be amplified by the electron wind, leading to a slit. SUO *et al.* (1993) suggested that this slit-forming is an instability phenomenon: a rounded cavity collapses into a slit at a critical electric field or a critical cavity radius, when the electron wind prevails over the surface tension.

The growth and coalescence of cavities may be assisted by dislocations, which act like pipes to transfer mass. Furthermore, core diffusion causes prismatic loops to climb. They buckle when the electron wind prevails over the dislocation line tension.

We will analyse cavities and prismatic loops together in this paper because of

their similarity. A formalism coupling dislocation mechanics and electromigration is presented in Section 2. The loop shape evolves according to an initial value problem, due to core diffusion, under the combined action of the electric field and line tension. Section 3 discusses the physical nature of buckling in the electron wind. We quantify the wind-capillarity competition by a dimensionless number. Section 4 formulates the governing equations for steady-state migration. Buckling and post-buckling states are analysed in Sections 5 and 6, respectively. The critical electric field is determined by finding the eigenvalues of the Mathieu equation. Section 7 interprets the above results for a cavity migrating and buckling due to surface diffusion, under the influence of an electric field and surface tension.

2. Electromigration-induced Dislocation Climb

Figure 1 illustrates a prismatic loop in the (X, Y) plane, with the Burgers vector b normal to the plane. Only a vacancy loop is considered; the results with a sign change are applicable to interstitial loops. Denote L as the dislocation length, and θ the angle of the normal vector. Atoms diffuse only along the dislocation core, driven simultaneously by the electric field component E_t tangent to the dislocation line, and by the chemical potential gradient $\mathrm{d}\mu/\mathrm{d}L$. The number of atoms per unit time passing a cross section of the core, i.e. the atomic flux, is given by the Einstein-type relation:

$$J_d = -\frac{D_d A_d}{\Omega k T}\left(Z_d^* e E_t + \frac{\mathrm{d}\mu}{\mathrm{d}L}\right), \tag{1}$$

where the subscript "d" refers to dislocation, $D_d A_d$ is the effective core diffusivity, Ω the volume per atom, k the Boltzmann constant, T the absolute temperature, e the electron charge, and Z_d^* (>0) the effective valence per atom in the core. The data for aluminum are given in Table 1. The effective valence Z_d^* is taken to be an average value reported for grain boundary electromigration.

The electric field E is applied along the X direction, its tangent component being

$$E_t = -E \sin\theta. \tag{2}$$

The chemical potential due to line tension Γ is (Friedel, 1964)

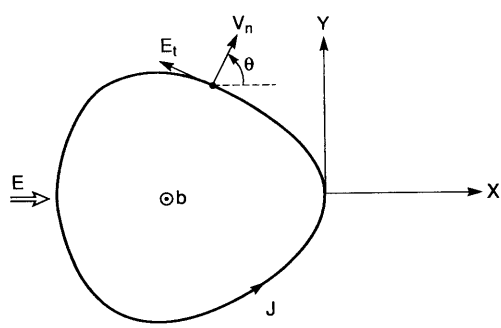

Fig. 1. A vacancy loop subjected to an electric field. The extra atomic plane lies outside of the loop.

TABLE 1. *Pure aluminum data*

Burgers vector	$b = 2.86 \times 10^{-10}$ m
Atomic volume	$\Omega = 1.66 \times 10^{-29}$ m^3
Shear modulus	$G = 2.54 \times 10^{10}$ N m^{-2}
Core diffusivity	$D_d A_d = 7.0 \times 10^{-25} \exp(-0.85\ \text{eV}/kT)$ m^4 s^{-1} (VOLIN *et al.*, 1971)
Effective valence	$Z_d^* = 20$

$$\mu = -K\Gamma\Omega/b. \tag{3}$$

Here K is the curvature, $K = \mathrm{d}\theta/\mathrm{d}L$. A constant line tension $\Gamma = \alpha G b^2$ is adopted in this paper, G being the shear modulus and $\alpha \approx 0.5$. The line tension is exactly constant for two important cases: a circular and a straight dislocation in an isotropic crystal. A numerical scheme similar to that of RAMIREZ *et al.* (1990) and ZHANG and YANG (1993) can compute the chemical potential for arbitrary dislocation shapes. This refinement will not be pursued here.

Mass conservation requires that

$$V_n = \frac{\Omega}{b}\frac{\mathrm{d}J_d}{\mathrm{d}L}, \tag{4}$$

where V_n is the climb velocity, positive if the extra atomic plane recedes. In time δt, the shape of the loop changes by

$$\delta X = V_n \cos\theta\delta t, \quad \delta Y = V_n \sin\theta\delta t. \tag{5}$$

The loop shape evolves according to (1)–(5), which defines an initial value problem. Given a current loop shape, the atomic flux is given by (1), and the climb velocity by (4); the shape is updated according to (5). The physical basis of the initial value problem is simple and well understood, but the solutions have a remarkable complex mathematical structure. This paper only explores the aspects of the problem which we believe to be of practical significance.

3. BUCKLING IN THE ELECTRON WIND

Several elementary considerations shed light on the nature of buckling in the electron wind. Only edge dislocations are discussed in this section; the conclusions, however, are applicable to cavities. First consider a straight dislocation in Fig. 2(a).

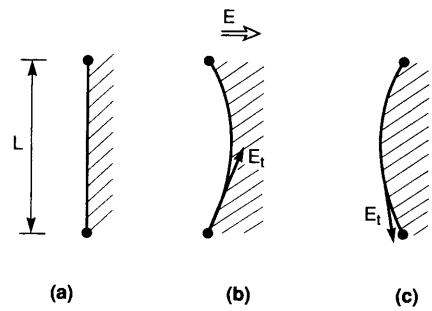

FIG. 2. Buckling of a straight dislocation. The extra atomic plane is shaded.

The two ends of the dislocation are pinned and immobile, but can be either atomic sinks or sources. The electric field is applied normal to the dislocation line. No force drives diffusion along the straight dislocation, so that the straight line is an equilibrium configuration. Yet this equilibrium configuration can be unstable: diffusion turns on as soon as the dislocation bends slightly. The atoms diffuse in the electron flow direction, i.e. in the direction opposing E_t. Figure 2(b) shows that E_t drives atoms to diffuse toward the two ends (atomic sinks), so that the extra atomic plane recedes. Figure 2(c) shows the opposite situation: E_t drives atoms to diffuse away from the two ends (atomic sources), so that the extra atomic plane extends. In both cases, the electron wind causes the dislocation to bend further. On the other hand, the line tension strives to straighten the dislocation. A dimensionless ratio quantifies the competition between the electron wind and the line tension (Suo, 1993):

$$\chi = \frac{Z_d^* eEbL^2}{\Gamma\Omega}. \tag{6}$$

The dislocation buckles when the electron wind prevails over the line tension, i.e. when χ exceeds a critical value χ_c. The analysis of Suo (1993) gave $\chi_c = \pi^2$. The buckled dislocation will evolve into either a vacancy thread [Fig. 2(b)], or an interstitial thread [Fig. 2(c)].

Next we consider a prismatic loop. A circular loop is in equilibrium if the line tension is isotropic. Furthermore, Suo (1993) showed that the loop translates with a circular shape under an applied electric field. However, the circular loop may be unstable. Figure 3 shows two non-circular loops, elongating either parallel the electric field (mode I), or normal to the electric field (mode II). Mode I has smaller curvature on the anode side than the cathode side, and the contrary is true for mode II. An inspection of this asymmetry reveals the essence of the instability: in each case, E_t is so directed that it will drive the core diffusion to *amplify* the asymmetry. Kraft *et al.* (1993) recognized similar behaviors after examining many cavities in electromigration tests. On the other hand, the line tensions strive to restore the circular symmetry. Consequently, the instability sets in when the electron wind prevails over the line tension. The wind–capillarity competition is governed by a similar dimensionless parameter

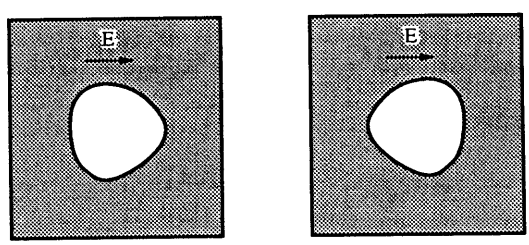

Fig. 3. Buckling of a circular loop. The extra atomic plane is shaded.

$$\chi = \frac{Z_d^* eEbR^2}{\Gamma\Omega}, \tag{7}$$

where R is the radius of the circle. If χ is small, the line tension dominates, and the dislocation loop is circular. If χ is large, the electron wind dominates, and the dislocation loop buckles into a noncircular shape. The circular loop loses the stability when χ exceeds a critical number χ_c, to be determined later. Note a size effect in this instability: only loops above a critical size will buckle under a given electric field. Similar dimensionless groups govern other electromigration instabilities, e.g. a loop breaking away from the precipitate (SUO, 1993).

4. STEADY-STATE MIGRATION

Compared with a straight dislocation, a circular loop has an additional complexity: it migrates even before it buckles. A complete analysis requires that the initial value problem in Section 2 be solved. In the electron wind, an initially circular loop, distorting and drifting, evolves into a noncircular shape, and then migrates with a fixed shape. That is, a steady-state, possible noncircular shape will emerge over a sufficiently long time. In what follows, we will avoid solving the transient problem, and focus on the steady-state motion. The general steady-state problem is formulated, followed by the pre-bifurcation, the bifurcation and the post-bifurcation solutions.

Figure 1 now represents a loop translating in a steady-state, i.e. every point on the loop translates at the same velocity in the X-direction, denoted as V. The coordinates also translate with the loop. The dislocation climb velocity is related to the loop translation velocity by

$$V_n = V\cos\theta. \tag{8}$$

Equations (1)–(4) and (8) lead to

$$\frac{\mathrm{d}}{\mathrm{d}\theta}\left(\kappa\frac{\mathrm{d}\kappa}{\mathrm{d}\theta}\right)+\eta\left(1-\frac{1}{\kappa}\right)\cos\theta = 0. \tag{9}$$

In deriving (9), we have used

$$\kappa = d\theta/dl, \quad \mathrm{d}x = -\sin\theta\,\mathrm{d}l, \quad \mathrm{d}y = \cos\theta\,\mathrm{d}l, \tag{10}$$

and normalized the lengths as

$$[X, Y, L, 1/K] = [x, y, l, 1/\kappa]\frac{D_d A_d}{\mathrm{k}TbV}Z_d^* eE. \tag{11}$$

The dimensionless group η is defined by

$$\eta = \left(\frac{D_d A_d}{\mathrm{k}TV}\right)^2\frac{(Z_d^* eE)^3}{\Gamma\Omega b}. \tag{12}$$

Equation (9) is the nonlinear ordinary differential equation that governs the steady-state shape.

The normalized curvature κ should vary with θ with period 2π. After κ is solved, the loop shape is integrated according to (10). To close a loop, x and y must also vary with θ with period 2π. This requires, according to (10), that

$$\int_0^{2\pi} \frac{\sin\theta\,\mathrm{d}\theta}{\kappa(\theta)} = 0, \quad \int_0^{2\pi} \frac{\cos\theta\,\mathrm{d}\theta}{\kappa(\theta)} = 0.$$

The second equation is implied by (9), as readily verified by integrating over 2π. The first equation is in general not satisfied by an odd periodic $\kappa(\theta)$, but satisfied by any even periodic $\kappa(\theta)$. Consequently, only even periodic $\kappa(\theta)$ will be of physical interest.

The steady-state equation (9) contains only one parameter, η. The solution of (9) does not depend on the radius of the initial circle. That is, the loop in a steady-state does not remember its evolution path—unless such memory is enforced somehow. Mass conservation requires the loop to enclose an invariant area. Thus, $\pi R^2 = -\oint X\,\mathrm{d}Y$, or in dimensionless form,

$$\chi = -\frac{\eta}{\pi}\oint x\,\mathrm{d}y. \tag{13}$$

Note that the right-hand side depends on η only, as solved from (9) and (10). Equation (13) determines the translation velocity at a given electric field.

The pre-buckling state is readily solved from (9); it is a circle with $\kappa = 1$. The translation velocity, determined by using either (13) or $K = 1/R$, is

$$V_0 = \frac{D_\mathrm{d}A_\mathrm{d}}{\mathrm{k}TRb}Z_\mathrm{d}^* eE. \tag{14}$$

Subscript 0 signifies the pre-buckling state. Thus, the circular loop migrating at a constant velocity is always a steady-state solution, and the line tension does not drive diffusion in this state. However, we will show that the circular loop is unstable above a critical electric field.

5. Bifurcation of a Circular Loop

Bifurcation is understood in the sense of Liapunov asymptotic stability. That is, a circular loop will bifurcate if a shape perturbation exists so that the loop will *never* return to the circular shape. The stability test requires that the transient problem be solved, which will not be pursued in this paper. Instead, we search for a noncircular, steady-state perturbation. Although the following mathematical analysis does not prove that such solutions are more stable than the circular loop, the instability of a circular loop is evident on the basis of the heuristic considerations in Section 3.

A small perturbation from the circular shape is

$$\kappa(\theta) = 1 + \varepsilon\kappa_1(\theta), \tag{15}$$

where ε is a small parameter, and $\kappa_1(\theta)$ a bifurcation mode. Substituting (15) into (9) and retaining only the first order terms in ε, one obtains that

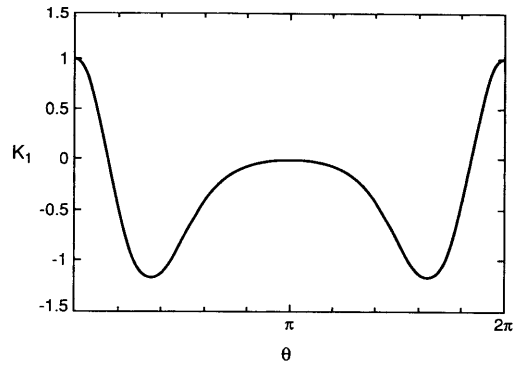

FIG. 4. Solution of the first order perturbation.

$$\frac{d^2\kappa_1}{d\theta^2} + \eta\kappa_1 \cos\theta = 0. \tag{16}$$

This is the Mathieu equation (MCLACHLAN, 1964); nontrivial, periodic, even solutions are sought. The lowest eigenvalue is $\eta = 10.65$, and the associated κ_1 is plotted in Fig. 4. Note that κ_1 times any number is also a solution. In particular, $\varepsilon > 0$ and $\varepsilon < 0$ corresponds, respectively, to the two modes in Fig. 3.

At the onset of the bifurcation, the translation velocity is identical to that of the circular loop. Thus, (7), (12) and (14) give the critical state quantities

$$\chi_c = 10.65, \tag{17}$$

$$E_c = 10.65\frac{\Gamma\Omega}{Z_d^* eR^2 b}, \tag{18}$$

$$V_c = 10.65\frac{D_d A_d \Gamma\Omega}{kTR^3 b^2}. \tag{19}$$

With the data in Table 1, a loop of radius $R = 1$ μm buckles at $E_c = 200$ V m^{-1}, and translates at $V_c = 2.2$ nm h^{-1} at $T = 500$ K. The critical electric field is within the range used in electromigration tests (typically $E = 100$–1000 V m^{-1}).

6. POST-BUCKLING SHAPES

We now examine post-bifurcation steady-states. Standard numerical methods are used to solve (9) for periodic even $\kappa(\theta)$ at various η. Painstaking care is needed to obtain the accurate solutions. After $\kappa(\theta)$ is obtained, the loop shape is integrated from (10), and χ from (13).

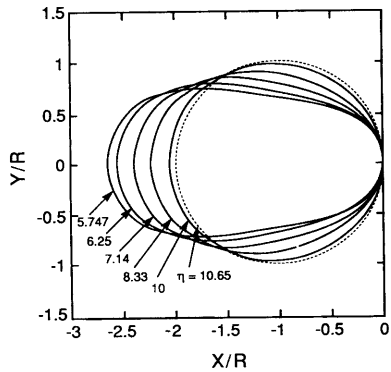

FIG. 5. Mode I steady-state shapes.

Figure 5 shows the mode I steady-state shapes. The loop migrates as a circle when $\eta = \chi$, buckles when $\eta = 10.65$, and finally becomes finger-like when η drops back to a smaller but definite value. The computation is terminated when the lowest curvature along the loop becomes infinitesimal. The η value obtained for that case approaches the infinitely long finger solution of SUO *et al.* (1994), $\eta = 5.743$. When interpreted as dislocation fingering, the latter predicts the fingering velocity

$$V = 0.417 \frac{D_d A_d}{kT} \frac{(Z_d^* eE)^{3/2}}{\sqrt{\Gamma \Omega b}}, \tag{20}$$

and the half-width of the finger

$$u = 2.40 \sqrt{\frac{\Gamma \Omega}{Z_d^* eEb}}. \tag{21}$$

Figure 6 shows plots of the mode II steady-state shapes, where the loops elongate normal to the electric field. Our numerical code proceeds for $\eta > 10.65$. The calculation terminates when $\kappa(0) \to 0$, which corresponds to $\eta = 14.91$.

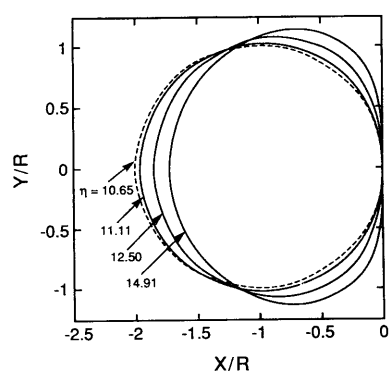

FIG. 6. Mode II steady-state shapes.

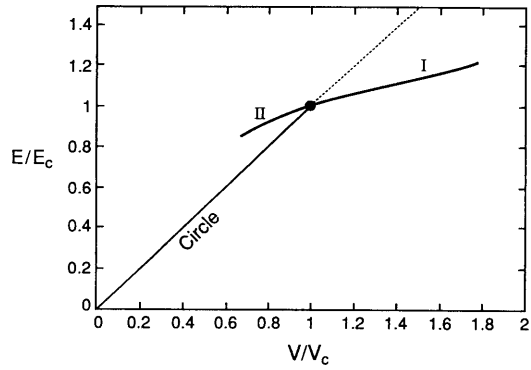

FIG. 7. Translation velocity versus the electric field.

The translation velocity as a function of the electric field is plotted in Fig. 7. They are normalized by the quantities at the bifurcation point, (18) and (19), respectively. The velocity increases linearly with the electric field up to the bifurcation point. After the loop buckles, a mode I loop migrates at higher velocity than a circular loop under the same electric field. According to (20), $V \propto E^{3/2}$ at high fields. This is because the finger-like loops have higher tangent component of the electric field. By contrast, a mode II loop migrates at a lower velocity than a circular loop under the same electric field, because the former has a lower tangent electric field component.

The total dislocation length L measures the deviation of the buckled shape from the circle. The length is integrated from (10) once the curvature is solved. Figure 8 shows the dislocation length as a function of the electric field. The loop length remains invariant before it buckles. A mode I loop elongates at a higher field. At high fields $E \gg E_c$, the width of the finger scales as $u \propto E^{-1/2}$, which implies that $L \propto E^{1/2}$ since the loop encloses an invariant area. A mode II loop elongates at a *lower* electric field, which indicates that the shape will continue to change after the circular loop buckles at a constant electric field $E = E_c$. The unstable disruption from a circle to a vertical finger signifies the catastrophic role of the electron wind. More complicated bifur-

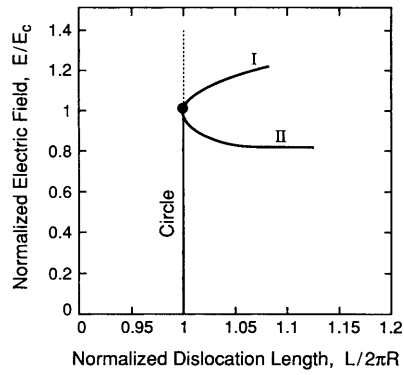

FIG. 8. The total length of the dislocation versus the electric field.

cation modes are possible, e.g. a loop may break into two loops, but will not be pursued in this paper.

The present formalism for dislocation climb in the electron wind is exact except for the line tension formula. The line tension is constant for circular loops. Thus we believe that the bifurcation state (17)–(19) is exact. Accuracy is questionable for other loop shapes; for example, the interaction between the parallel dislocation lines may cause secondary buckling, multiplying smaller loops (Suo, 1993). These subtleties aside, we believe that the essence of dislocation buckling discussed in Section 3 prevails even if the line tension formula (3) is inaccurate. Implications of prismatic loop migration and multiplication for electromigration damage have been discussed by Suo (1993).

7. A Cavity Collapses into a Slit in the Electron Wind

Now we consider a cavity collapsing in an infinite, isotropic crystal subjected to an electric field. The qualitative analysis of Section 3 is valid for the cavity buckling, with core diffusion replaced by surface diffusion, and line tension by surface tension. Let γ_s be the surface energy, $Z_s^*(>0)$ the effective valence for each atom on the metal surface, R the radius of the circular cavity, E the applied electric field. The relative importance of the surface energy and the electron wind is described by a similar dimensionless group

$$\chi_s = \frac{Z_s^* eER^2}{\gamma_s \Omega}. \tag{22}$$

If χ_s is small, the surface energy dominates, and the cavity retains the circular shape as it drifts in the electron wind. If χ_s is large, the electric field dominates, and the cavity buckles to a noncircular shape. Similar dimensionless groups govern other electromigration instabilities, such as a cavity or a precipitate penetrating a grain boundary (Li *et al.*, 1992; Ma and Suo, 1993).

Yet a new feature appears, namely, the electric current is crowded around the cavity. Because of the relatively low electric field and temperature in electromigration tests, negligible electrons are emitted from the metal surface and the medium inside the cavity does not break down. Consequently, the cavity is a perfect insulator inside an interconnect. The electric field around the cavity can be determined by the Laplace equation governing the electric potential, ϕ. Let L be the arclength on the surface. Once ϕ is determined, the tangential electric field is given by $E_t = -\mathrm{d}\phi/\mathrm{d}L$. Numerical analysis is needed in general. In what follows we outline the problem and present an estimate of the buckling condition.

Both the electron wind and surface energy drive atoms to diffuse on the cavity surface:

$$J_s = -\frac{D_s \delta_s}{\Omega k T}\left(Z_s^* eE_t + \frac{\mathrm{d}\mu}{\mathrm{d}L}\right). \tag{23}$$

Here J_s is the surface flux of atoms (numbers of atoms per length per time), $D_s\delta_s$ the

effective surface diffusivity. The chemical potential due to the surface tension is $\mu = -\Omega\gamma_s K$, where K is the curvature on the cavity surface (HERRING, 1951).

Conservation of atoms sets a kinematic constraint: at any point the surface recedes if the flux has a positive divergence, i.e.

$$V_n = \Omega\, \partial J_s/\partial L. \tag{24}$$

Here $V_n = \mathbf{n}\cdot\partial\mathbf{X}/\partial t$ is the normal velocity of the surface, where t is the time, $\mathbf{X}$ the position vector of a point on the surface, and $\mathbf{n}$ the unit vector normal to the surface pointing into the solid; $V_n > 0$ if the surface recedes.

For a circular cavity in an infinite lattice subjected to a remote electric field E, the electric field inside the cavity is uniform and of magnitude $2E$. Thus,

$$E_t = -2E\sin\theta. \tag{25}$$

The factor of 2 reflects the current crowding in the metal caused by the insulating cavity. The analogy between a prismatic loop and a cavity is evident when compared with Section 2. A circular cavity migrating at constant velocity

$$V_0 = 2\frac{D_s\delta_s}{kTR}Z_s^* eE \tag{26}$$

is a steady-state solution. Note the factor of 2 difference from its counterpart for a prismatic loop (14). This result is the same as that obtained by HO (1970).

The buckling condition cannot be rigorously obtained by this analogy. As evident from the qualitative discussion in Section 3, the buckling shape should be a curved triangle. The detailed buckling shape of the cavity is expected to differ from that of the dislocation loop, because the change in the cavity shape induces a change in the electric field near the cavity. For example, the electric field inside the cavitiy will no longer be uniform. To rigorously determine the buckling condition, one has to iterate the cavity shape and solve the Laplace equation for the electric potential for each cavity shape. This problem will not be pursued in this paper. Instead, we simply use the analogous result (17), and include the factor of 2 difference for the current crowding around the cavity. Thus, the circular cavity buckles when

$$\frac{Z_s^* eER^2}{\gamma_s\Omega} = 5.325. \tag{27}$$

We emphasize that the numerical value in (27) is not obtained by rigorous analysis. Yet the dimensionless group is correct, and we believe that the result can be used to estimate the order of magnitude. Using $Z_s^* = 20$, $\gamma_s = 1\ \mathrm{J\ m^{-2}}$, one finds that the critical radius is $R = 226$ nm under electric field $E = 540\ \mathrm{V\ m^{-1}}$. The predicted magnitudes are consistent with those observed experimentally by KRAFT *et al.* (1993) and ROSE (1992).

The mode I post-buckling has been studied by SUO *et al.* (1993) in the limiting case of a long finger in the electric field direction. Yet more relevant to interconnect reliability is the mode II post-buckling, where slits grow normal to the electric field, across the linewidth. The current is more crowded as the cavity elongates normal to the field direction. The problem should be solved by numerically determining the

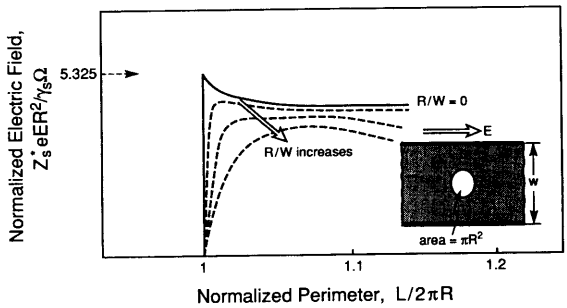

FIG. 9. A cavity collapses into a slit in an aluminum interconnect.

electric field first. However, many apparent complications fall away once the basic underlying pattern is discovered. Figure 9 sketches the anticipated mode II solution from such an analysis. The linewidth w introduces a dimensionless number R/w, which can be viewed as an imperfection in the standard bifurcation theory. The case $R/w = 0$ corresponds to a cavity in an infinite interconnect. The cavity starts to deviate from the circular shape at any finite electric field when $R/w \neq 0$, but the curves are expected to follow the trend indicated in Fig. 9. Surface energy anisotropy can also be viewed as an imperfection, causing the cavity to be noncircular even before the electric field turns on.

8. Concluding Remarks

A rounded cavity collapses into a slit at a critical electric field or a critical radius. The shape instability is due to surface diffusion when the electron wind prevails over the surface tension. Although this phenomenon is very new, it is useful to place it into perspective, on the basis of the available experimental evidence and theoretical insight. A passivated interconnect is limited in atomic sinks, hillocks being suppressed. Cavity growth requires long-range mass transport, and thereafter takes a long time. On the other hand, it takes a short time for a slit to cross the linewidth after the instability sets in. Consequently, an interconnect is likely to spend most of its lifetime in growing a rounded void to a critical size. The critical size is given by (25) for a cavity in an infinite interconnect, which is one of the important factors that set the interconnect lifetime. However, the evolution details *after* the cavity buckles are probably inconsequential to the lifetime. Further attention should be directed toward nucleation and growth of rounded cavities, so that the major part of the lifetime can be predicted. The size effect in this instability implies that slit will not form if the electric field is low, or the linewidth is small. This places a limit on the empirical approach: lines of different widths under different electric fields may fail in different ways. The significance of prismatic loops as mass-carriers in electron wind has been discussed by Suo (1993). Post-bifurcation solutions in this paper show that a finger-like dislocation can extend under electric fields in the range of typical electromigration tests.

ACKNOWLEDGEMENTS

We wish to thank Professor E. Arzt of the Max-Planck-Institut at Stuttgart, and Dr J. E. Sanchez of Advanced Micro Devices for bringing the transgranular slit problem to our attention, and a reviewer for pointing out a flaw in the original manuscript, which leads to the cautionary remarks in the paragraph containing equation (27). W. Yang was supported by a visiting appointment at the University of California, Santa Barbara, funded by the Office of Naval Research through contract N00014-93-1-0110, and by the National Natural Science Foundation of China. The work was supported by the National Science Foundation through grant MSS-9202165, and through a Young Investigator Award MSS-9258115 to Z. Suo.

REFERENCES

ARZT, E. and NIX, W. D. (1991) A model for the effect of line width and mechanical strength on electromigration failure of interconnects with "near-bamboo" grain structures. *J. Mater. Res.* **6,** 731–736.

FRIEDEL, K. (1964) *Dislocations*. Pergamon Press, Oxford.

GENUT, M., LI, Z., BAUER, C. L., MAHAJAN, S., TANG, P. F. and MILNES, A. G. (1991) Characterization of the early stages of electromigration at grain boundary triple junctions. *Appl. Phys. Lett.* **58,** 2354–2356.

HERRING, C. (1951) Surface tension as a motivation for sintering. *The Physics of Powder Metallurgy* (ed. W. E. KINGSTON), pp. 143–179. McGraw-Hill, New York.

HO, P. S. (1970) Motion of inclusion induced by a direct current and a temperature gradient. *J. Appl. Phys.* **41,** 64–68.

HO, P. S. and KWOK, T. (1989) Electromigration in metals. *Rep. Prog. Phys.* **52,** 301–348.

JOO, Y.-C. and THOMPSON, C. V. (1993) Evolution of electromigration-induced voids in single crystalline aluminum lines with different crystallographic orientations. *Mater. Res. Soc. Symp. Proc.* **309,** 351–356.

KIRCHHEIM, R. (1992) Stress and electromigration in Al-lines of integrated circuits. *Acta Metall. Mater.* **40,** 309–323.

KORHONEN, M. A., BØRGESEN, P., TU, K. N. and LI, C.-Y. (1993) Stress evolution due to electromigration in confined metal lines. *J. Appl. Phys.* **73,** 3790–3799.

KRAFT, O., BADER, S., SANCHEZ, J. E. and ARZT, E. (1993) Observation and modeling of electromigration-induced void growth in Al-based interconnects. *Mater. Res. Soc. Symp. Proc.* **309,** 199–204.

LI, C.-Y., BØRGESEN, P. and KORHONEN, M. A. (1992) Electromigration-induced failure in passivated aluminum-based metallizations—the dependence on temperature and current density. *Appl. Phys. Lett.* **61,** 411–413.

LLOYD, J. R. (1991) Electromigration failure. *J. Appl. Phys.* **69,** 7601–7604.

MA, Q. and SUO, Z. (1993) Precipitate drifting and coarsening caused by electromigration. *J. Appl. Phys.* **74,** 5457–5462.

MCLACHLAN, N. W. (1964) *Theory and Application of Mathieu Functions*. Dover Pub., New York.

RAMIREZ, J.-C., BOWER, A. and FREUND, L. B. (1990) Simulation of transient glide of a treading dislocation in an embedded strained epitaxial layer. Brown University Report.

ROSE, J. H. (1992) Fatal electromigration voids in narrow alumin-copper interconnect. *Appl. Phys. Lett.* **61,** 2170–2172.

SANCHEZ, J. E., MCKNELLY, L. T. and MORRIS, J. W. (1992) Slit morphology of electromigration induced open circuit failures in fine line conductors. *J. Appl. Phys.* **72,** 3201–3203.

SHINGUBARA, S. and NAKASAKI, Y. (1991) Electromigration in a single crystalline submicron width aluminum interconnection. *Appl. Phys. Lett.* **58,** 42–44.

Suo, Z. (1993) Electromigration-induced dislocation climb and multiplication in conducting lines. *Acta Metall. Mater.* In press.

Suo, Z., Wang, W. and Yang, M. (1994) Electromigration instabilities: transgranular slits in interconnects. *Appl. Phys. Lett.* **64**(15).

Thompson, C. V. and Lloyd, J. R. (1993) Electromigration and IC interconnects. *MRS Bulletin* December 1993, pp. 19–25.

Totta, P. A. (1991) Stress-induced phenomena in metallizations: U.S. perspective. *Stress-Induced Phenomena in Metallization* (eds C. Y. Li, P. Totta and P. Ho), pp. 1–20. American Institute of Physics, New York.

Volin, T. E., Lie, K. H. and Balliffi, R. W. (1971) Measurement of rapid mass transport along individual dislocations in aluminum. *Acta Metall.* **19,** 263–274.

Zhang, H. and Yang, W. (1993) Three dimensional dislocation loops generated from a weak inclusion in a strained material heterostructure. *J. Mech. Phys. Solids* **42,** 913–930.